ISSN 1674-1056
http://cpb.iphy.ac.cn
http://iopscience.iop.org/cpb
中国物理 B
Chinese Physics
中国物理 Chinese Physics B

Controllable laning phase for oppositely driven disk systems

Lin Liu(刘琳)[1], Ke Li(李珂)[1], Xiao-Lin Zhou(周晓琳)[1], Lin-Li He(何林李)[2], Lin-Xi Zhang(章林溪)[1]
Citation: Chin. Phys. B . 2019, 28(12): 120501 . **doi:** 10.1088/1674-1056/ab4e86
Journal homepage: http://cpb.iphy.ac.cn; http://iopscience.iop.org/cpb

What follows is a list of articles you may be interested in

Role of entropy generation minimization in thermal optimization

Xue-Tao Cheng(程雪涛), Xin-Gang Liang(梁新刚)
Chin. Phys. B . 2017, 26(12): 120505 . **doi:** 10.1088/1674-1056/26/12/120505

Spurious symmetry-broken phase in a bidirectional two-lane ASEP with narrow entrances

Bo Tian(田波), Rui Jiang(姜锐), Mao-Bin Hu(胡茂彬), Bin Jia(贾斌)
Chin. Phys. B . 2017, 26(2): 020503 . **doi:** 10.1088/1674-1056/26/2/020503

Analyses of an air conditioning system with entropy generation minimization and entransy theory

Yan-Qiu Wu(吴艳秋), Li Cai(蔡黎), Hong-Juan Wu(吴鸿娟)
Chin. Phys. B . 2016, 25(6): 060507 . **doi:** 10.1088/1674-1056/25/6/060507

Entransy analyses of heat-work conversion systems with inner irreversible thermodynamic cycles

Cheng Xue-Tao, Liang Xin-Gang
Chin. Phys. B . 2015, 24(12): 120503 . **doi:** 10.1088/1674-1056/24/12/120503

Performance characteristics of low-dissipative generalized Carnot cycles with external leakage losses

Huang Chuan-Kun, Guo Jun-Cheng, Chen Jin-Can
Chin. Phys. B . 2015, 24(11): 110506 . **doi:** 10.1088/1674-1056/24/11/110506

Controllable laning phase for oppositely driven disk systems*

Lin Liu(刘琳)[1], Ke Li(李珂)[1], Xiao-Lin Zhou(周晓琳)[1], Lin-Li He(何林李)[2,†], and Lin-Xi Zhang(章林溪)[1,‡]

[1] *Department of Physics, Zhejiang University, Hangzhou* 310027, *China*
[2] *Department of Physics, Wenzhou University, Wenzhou* 325035, *China*

(Received 10 August 2019; revised manuscript received 17 September 2019; published online 22 November 2019)

A two-dimensional binary driven disk system embedded by impermeable tilted plates is investigated through nonequilibrium computer simulations. It is well known that a binary disk system in which two particle species are driven in opposite directions exhibits jammed, phase separated, disordered, and laning states. The presence of tilted plates can not only advance the formation of laning phase, but also effectively stabilize laning phase by suppressing massively drifting behavior perpendicular to the driving force. The lane width distribution can be controlled easily by the interplate distance. The collective behavior of driven particles in laning phase is guided by the funnel-shaped confinements constituted by the neighboring tilted plates. Our results provide the important clues for investigating the mechanism of laning formation in driven system.

Keywords: driven system, tilted plates, laning phase, drifting behavior

PACS: 05.70.Ln, 66.10.cd, 87.18.Gh, 05.70.–a **DOI:** 10.1088/1674-1056/ab4e86

1. Introduction

Far from thermodynamic equilibrium, nonequilibrium system often exhibits a series of fascinating phase transitions along with unusual pattern formation and novel transport properties,[1,2] especially in driven diffusive systems.[3,4] For example, the oppositely charged colloidal mixtures driven by an electric field will undergo a nonequilibrium phase transition from a disordered state into a dynamically ordered state, such as sliding crystal or sliding smectic.[5,6] One of the most striking dynamical behaviors is a transition to lane formation, where particles of the same kind move collectively in the direction parallel to the field direction, and high mobility is achieved through organization of the particles into noncolliding chains.[7–10] Such a nonequilibrium transition towards lane formation is a general phenomenon occurring in dusty plasmas,[11,12] granular matter,[13] as well as in active matter composed of autonomously moving agents such as pedestrians,[14,15] social insects,[16] bacteria and cells,[17,18] and artificial colloidal microswimmers.[19]

Recently, a lot of experimental,[6] theoretical,[20,21] and simulation[7,22–24] studies have been devoted to investigating the lane formation in mixtures of oppositely driven particles. Dzubiella *et al.* investigated this issue by experimental means and Brownian dynamics simulations. They put forward a dynamical criterion for judging the lane formation: there is an enhanced lateral mobility of particles induced by collisions with particles driven in the opposite direction, which sharply decreases once lanes are formed. Therefore, particles in a lane can be regarded as being in a dynamically 'locked-in' state.[7,8,23] Chakrabarti *et al.* used the dynamic density-functional theory to argue that the Langevin dynamics of oppositely driven particles implies laning via a dynamic instability of the homogenous phase.[20,21] Samuel *et al.* studied the mixtures of self-propelled particles in a two-dimensional (2D) particle system by using Brownian dynamics simulations. The simulations demonstrated that the two species spontaneously segregate to generate a rich array of dynamical domain structures whose properties depend on the propulsion velocity, density, and composition.[22] Reichhardt *et al.* numerically examined a 2D particle system in which two particle species are driven in opposite directions. For particle density $\Phi < 0.55$ and increasing the drive force, they identified four dynamical phases, *i.e.*, a crystalline jammed phase, a fully phase separated state, a strongly fluctuating liquid phase, and a laning phase or smectic state. The transitions between these different phases are associated with jumps or dips in the velocity–force curves and the differential mobility along with global changes in the structural order of the system.[23–25] In their other work, they simulated a laning system containing active disks that obey run-and-tumble dynamics, and identified a novel drive-induced clustered laning state that remains stable even at density below the activity-induced clustering transition of the undriven system.[26]

The formation of lanes with high moving velocity can accelerate particle transport along the field direction but suppress massively transport perpendicular to the field. There-

*Project supported by the National Natural Science Foundation of China (Grant Nos. 21873082, 21674082, and 21674096) and the Natural Science Foundation of Zhejiang Province, China (Grant No. LY19B040006).

†Corresponding author. E-mail: linlihe@wzu.edu.cn
‡Corresponding author. E-mail: lxzhang@zju.edu.cn

© 2019 Chinese Physical Society and IOP Publishing Ltd

fore, laning transition is expected to be widely used in type-II superconductors,[27,28] electron crystals, such as electronic ink and electrophoresis in microfluidics, and even as a concept of panic theory applied to pedestrian zones.[29] Nevertheless, the nature of laning transition is still being debated and key variables have not been characterized yet. Meanwhile, in most cases, the dynamical lane is unstable and non-uniform with drifting defects. In order to obtain the stable laning phase, where the lane width can be controlled and tailored freely, in this paper, we focus on a 2D particle system in which two particle species are driven in opposite directions. In the absence of confinement or obstacle, such a system is known to exhibit four dynamical phases, *i.e.*, a jammed phase with no motion, a fully phase-separated state with high-mobility, a disordered fluctuating state with lower mobility, and a laning phase in a free flow.[8,30] Then embedding tilted plates into the 2D driven particle system can effectively stabilize laning phase by suppressing massively drifting behavior perpendicular to the driving force.[31] Finally, lane width and distribution can be controlled freely by the interplate distance and the orientation of the tilted plates, respectively. These results can provide important clues for investigating the mechanism and application of laning formation in driven systems.

2. Model and method

We numerically simulate a 2D disk system of size $L \times L$ with periodic boundary conditions in the x and y directions, containing N_d disks of radius R_d. Here $L = 30$ and $R_\mathrm{d} = 0.5$. The particle density Φ is defined as the number of particles divided by the area coverage of the disks, *i.e.*, $\Phi = N_\mathrm{d}\pi R_\mathrm{d}^2/L^2$. Reichhardt *et al.* studied a binary system of two disks driven in opposite directions, and revealed four dynamic phases, *i.e.*, a jammed state (phase I), a fully phase separated state (phase II), a mixed or disordered state (phase III), and a laning state (phase IV). Their results showed that the system is always in a laning state for particle density $\Phi < 0.55$, while the disks can organize into more than four dynamic phases for $\Phi \geq 0.55$.[23] In our study, $\Phi = 0.82$. In addition, N immobile plates with a certain tilt angle θ are embedded into a 2D driven disk system with $\theta = 10^\circ$. The simple model is shown in Fig. 1. In the uniform case, the interplate distance d_i is defined by L/N, where N varies from $N = 0$ to $N = 6$ in our work. Of course, the interplate distance d_i can also be freely set to be a certain value. The embedded plate is composed of m_p particles (here $m_\mathrm{p} = 13$) with a fixed distance R_p between consecutive particles. Here $R_\mathrm{p} = 0.5$, which is equal to the disk radius R_d.

The dynamics of disk i obeys the overdamped equation of motion as follows:

$$\eta \frac{\mathrm{d}\boldsymbol{R}_i}{\mathrm{d}t} = \boldsymbol{F}^i_\mathrm{dd} + \boldsymbol{F}^i_\mathrm{dp} + \boldsymbol{F}^i_\mathrm{D}. \tag{1}$$

Here, η is the damping constant and $\boldsymbol{R}_i$ is the location of disk i. The disk–disk and disk–plate interactions are modeled as a finite range repulsive harmonic spring. The disk–disk interaction force is

$$\boldsymbol{F}_\mathrm{dd} = \sum_{i\neq j}^{N_\mathrm{d}} k_1 \left(2R_\mathrm{d} - |\boldsymbol{r}_{ij}|\right) \Theta\left(2R_\mathrm{d} - |\boldsymbol{r}_{ij}|\right)\hat{\boldsymbol{r}}_{ij},$$

where $\boldsymbol{r}_{ij} = \boldsymbol{R}_i - \boldsymbol{R}_j$, $\hat{\boldsymbol{r}}_{ij} = \boldsymbol{r}_{ij}/|\boldsymbol{r}_{ij}|$, and Θ is the Heaviside step function. Here the spring constant $k_1 = 60$. The disk–plate interaction is

$$\boldsymbol{F}_\mathrm{dp} = \sum_{\mathrm{p}=1}^{N_p} k_2 \left(2R_\mathrm{d} - |\boldsymbol{r}_{i\mathrm{p}}|\right) \Theta\left(2R_\mathrm{d} - |\boldsymbol{r}_{i\mathrm{p}}|\right)\hat{\boldsymbol{r}}_{i\mathrm{p}},$$

where $N_\mathrm{p} = N \times m_\mathrm{p}$, $\boldsymbol{r}_{i\mathrm{p}} = \boldsymbol{R}_i - \boldsymbol{R}_\mathrm{p}$, $\hat{\boldsymbol{r}}_{i\mathrm{p}} = \boldsymbol{r}_{i\mathrm{p}}/|\boldsymbol{r}_{i\mathrm{p}}|$, and $k_2 = 800$. Each disk is subjected to an applied driving force, $F^i_\mathrm{D} = A^i F_\mathrm{D}\hat{\boldsymbol{x}}$, where N_1 disks are driven in the positive x direction with $A^i = 1.0$, and the remaining $N_2 = N_\mathrm{d} - N_1$ disks are driven in the negative x direction with $A^i = -1.0$. Here, $N_2 = N_1$. After applying the drive force, the systems are run at least 1×10^7 simulation time steps to ensure it can reach a steady state. Then we measure the average disk velocity for each species and normalize it by $N_{1(2)}$ to obtain the average velocity per disk $\langle V_{1(2)}\rangle = N^{-1}_{1(2)} \sum_{i=1}^{N_{1(2)}} \boldsymbol{V}_i\hat{\boldsymbol{x}}$, where $\boldsymbol{V}_i$ is the instantaneous velocity of disk i. In our study, with damping constant of $\eta = 1.0$, the overdamped dynamics of system is in the free flow limit and then the disks move at a velocity of $\langle V_1\rangle = F_\mathrm{D}$ and $\langle V_2\rangle = -F_\mathrm{D}$.

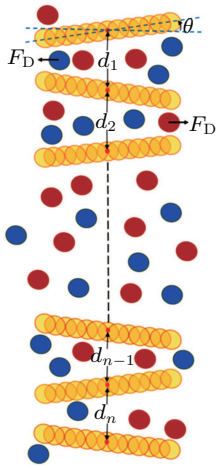


Fig. 1. Simple model of tilted plates with angle θ embedded in a 2D disk system, with d_i ($i = 1, 2, \ldots, n$) denoting interplate distance between two adjacent tilted plates. Here $\theta = 10^\circ$, red disks (specie A) are driven in $+x$ direction, and blue disks (specie B) are driven in $-x$ direction.

3. Result and discussion

Firstly, we compare the binary driven disk systems without ($N = 0$) and with ($N = 2$ and 4) tilted plates. Figures 2(a)–2(c) display the specie A average velocity $\langle V_A\rangle$, $\mathrm{d}\langle V_A\rangle/\mathrm{d}F_\mathrm{D}$, and the fraction of sixfold coordinated particles P_6, as a function of F_D, respectively. Here $P_6 = N_\mathrm{d}^{-1} \sum_{i=1}^{N_\mathrm{d}} \delta(z_i - 6)$, where

z_i is the coordination number of particle i obtained from a Voronoi construction.[24] The above velocity–force curves indicate that they also have four distinct dynamical phases: a crystalline jammed phase I, a fully phase separated state II, a strongly fluctuating liquid phase III, and a laning phase IV. The curve of $\mathrm{d}\langle V_A\rangle/\mathrm{d}F_\mathrm{D}$ further indicates the transition points between these dynamical phases, as well as P_6 characterizes the disk ordering and the nature of the dynamic fluctuations.

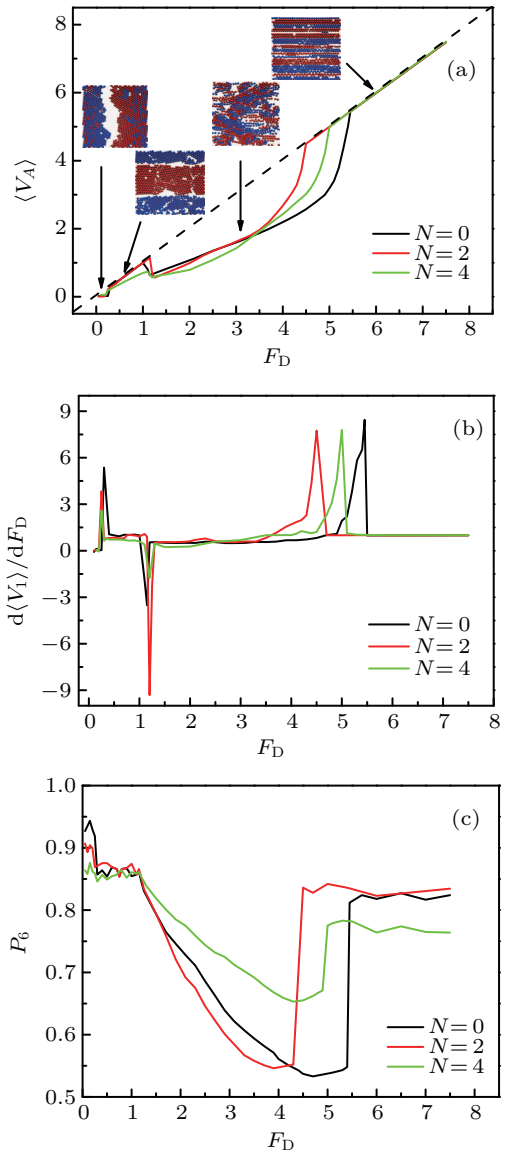


Fig. 2. Plots of (a) $\langle V_A\rangle$, (b) $\mathrm{d}\langle V_A\rangle/\mathrm{d}F_\mathrm{D}$, and (c) P_6 *versus* F_D for three different values of N.

In general, the potential energy initially increases and then decreases towards its steady-state limit. That means that starting from a mixed configuration at time $t = 0$, the opposite drive increases the separation between particles of different species, which increases the potential energy while subsequent laning causes these energetically consumed collisions to decrease.[8,32] Now taking $N = 0$ for example, the jammed state (phase I) is located in the range of $0 < F_\mathrm{D} < 0.3$ with $\langle V_\mathrm{A}\rangle = 0$, indicating that disks are stuck with no motion. Correspondingly, $P_6 \approx 0.92$, indicating that the system has a strong sixfold disk ordering. Within phase I, the disks form a dense cluster with triangular order as shown in the disk configuration by Fig. 3(a) for $F_\mathrm{D} = 0.1$. In our system, $\Phi = 0.82$, which is below the jammed limit, therefore $P_6 < 1.0$ due to the disks on the edge of the jammed cluster with no six neighbors. The first peak in $\mathrm{d}\langle V_A\rangle/\mathrm{d}F_\mathrm{D}$ curve occurs at $F_\mathrm{D} = 0.3$, indicating the transition from phase I to phase II. The phase separated state (phase II) appears in the range of $0.3 < F_\mathrm{D} < 1.15$ with $\langle V_A\rangle$ increasing linearly with F_D and $\mathrm{d}\langle V_A\rangle/\mathrm{d}F_\mathrm{D} = 1.0$, meaning that the particles are in a free flow regime. Meanwhile, both species are separated in phases and exhibit a triangular ordering with $P_6 \approx 0.86$ as shown in Fig. 3(a) at $F_\mathrm{D} = 0.7$. Surprisingly, a negative peak in $\mathrm{d}\langle V_A\rangle/\mathrm{d}F_\mathrm{D}$ curve appears at $F_\mathrm{D} = 1.15$ coinciding with the transition from phase II to phase III. In phase III, particle collision frequency increases, causing a large amount of energy loss for the whole system and lowering the mobility.[26,33] This is a typical example of negative differential mobility where the particle average velocity decreases with driving force increasing. In the system with quenched disorder, the negative differential mobility has also been observed at transition from ordered to disordered or turbulent flow phase as a function of increasing drive.[32,33]

The strongly fluctuating liquid state (phase III) takes up the range of $1.15 < F_\mathrm{D} < 5.45$, accompanied by a sharp drop in P_6, illustrating that the system enters into the disordered flow phase. In phase III, two particle species continuously collide with each other, leading to a massive velocity loss in the y direction, transverse to the drive direction. Finally, two particle species are intensively mixed as shown in Fig. 3(a) for $F_\mathrm{D} = 4.5$. Another positive peak in $\mathrm{d}\langle V_\mathrm{A}\rangle/\mathrm{d}F_\mathrm{D}$ curve appears at $F_\mathrm{D} = 5.45$, corresponding to the transition from phase III to phase IV. The laning state (phase IV) is observed when $F_\mathrm{D} > 5.45$ with $\mathrm{d}\langle V_\mathrm{A}\rangle/\mathrm{d}F_\mathrm{D} = 1.0$, demonstrating that the particles are in a free flow regime. As shown in Fig. 3(a) at $F_\mathrm{D} = 7.5$, the disks form multiple oppositely moving lanes. Meanwhile, the system exhibits a triangular ordering again with P_6 going back to $P_6 \approx 0.82$. These results of the binary driven disk system ($N = 0$), are completely consistent with the studies by Reichhardt *et al.*[22,23]

Then we turn to the binary driven disk systems embedded with tilted plates,[34,35] such as $N = 2$ and 4. There are also four typical dynamical phases mentioned above, especially in the case of $N = 4$ shown in Fig. 3(c). From Figs. 2 and 3, we can see that the III–IV transitions occur at $F_\mathrm{D} = 4.5$ for $N = 2$ and $F_\mathrm{D} = 5.0$ for $N = 4$, both are lower than $F_\mathrm{D} = 5.45$ for $N = 0$. This result indicates that the presence of tilted plates does not change the dynamical phase transition but can lower the critical driving force at which the dynamical III–IV transition occurs, and advance the formation of laning phase. A

closer look at Fig. 3(b) shows the jammed and phase separated states (phases I and II) depend on a competition between two effects: the internal interaction force between the particles, and the external driving force, irrelevant to the tilted plates. In laning formation (phase IV), there appear two different configurations with driving force increasing, named laning-*A* and laning-*B* phases, respectively. At $F_{\rm D} = 4.5$, the laning-*A* phase looks similar to phase II, but essentially is completely different from it, which is uniformly divided into two lanes induced by two plates. At $F_{\rm D} = 7.5$, the laning-*B* phase is formed as the high driving force, independent of the tilted plates, similar to the laning phase without plates as shown in Fig. 3(a). For $N = 4$ at $F_{\rm D} = 7.5$, laning-*A* phase is also uniformly divided into four lanes by four plates. Of course, as driving force reaches a certain value, the inducing effects of the tilted plates will fail, and system is finally settled into laning-*B* phase. As a result, a regular and uniform laning-*A* phase characterized lane width, which will be discussed below in detail, can be obtained by the tilted plates if the external driving force does not exceed a critical strength. As is well known, a static confinement or obstacle is shown to be able to accumulate and collect driven particles and trapping devices. This collective effect can be used to guide or rectify the motion of microbes and man-made microswimmers in a controlled way.[36,37] Here, neighboring tilted plates can be regarded as funnel-shaped confinements one by one. The funnels can first guide the collective behaviors of the same driven particles to the direction of the cusp of funnels. Once particles are in a lane, transverse diffusivity is further suppressed by two plates and ordered laning phase is formed.

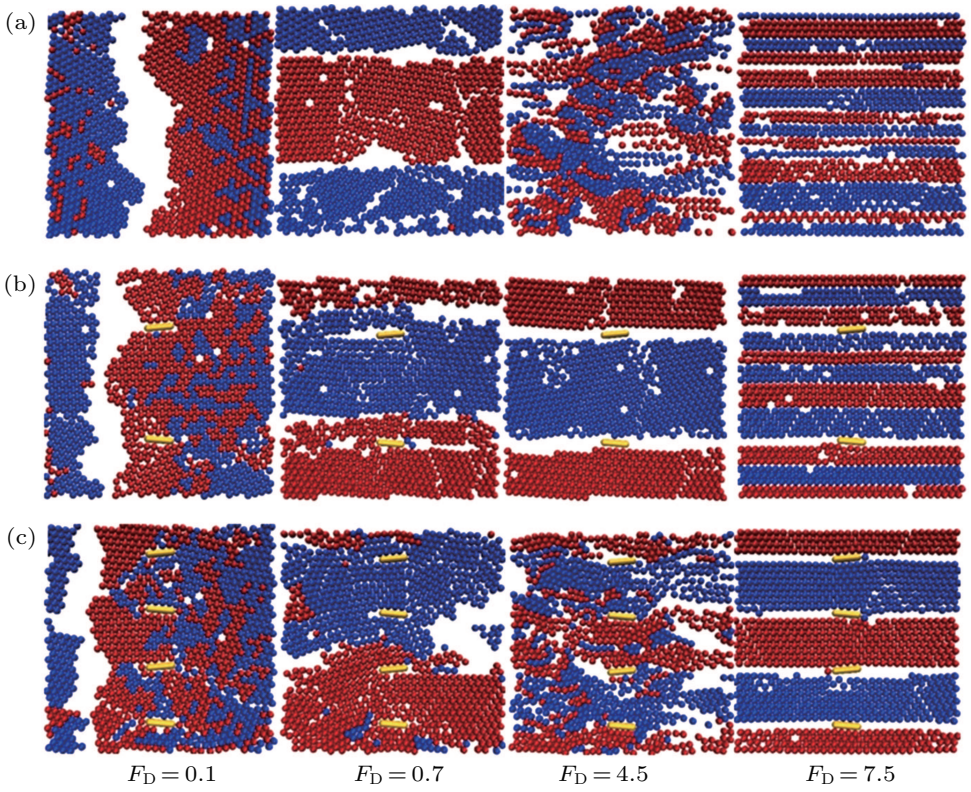


Fig. 3. Disk configurations for three cases with different values of $F_{\rm D}$ for $N = 0$ (a), 2 (b), and 4 (c).

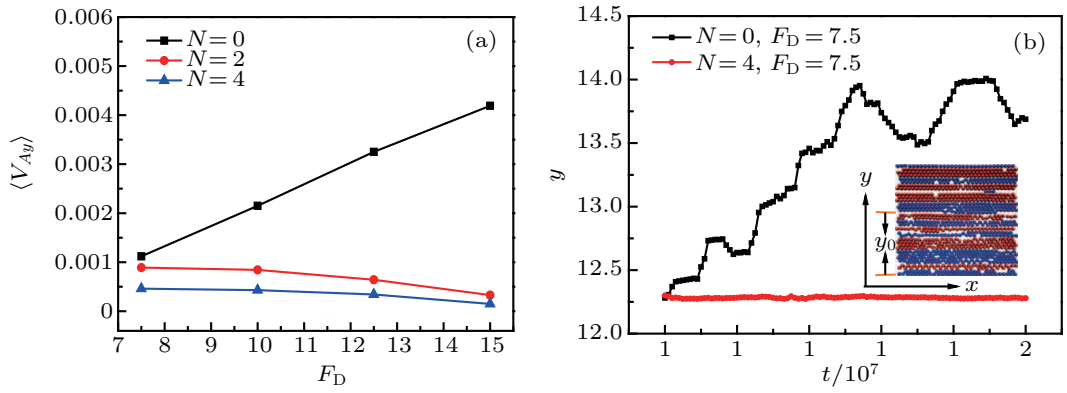


Fig. 4. (a) Plots of average velocity of species *A* disk in direction $\langle V_{Ay} \rangle$ *versus* $F_{\rm D}$ for three different values of N, and (b) time-dependent y coordinate of selected disk with initial y_0 coordinate for $F_{\rm D} = 7.5$.

Next, we focus on the laning phase with $F_D \geq 7.5$ for two cases without and with tilted plates. Here the species A average velocity in the y direction $\langle V_{Ay} \rangle$ as a function of F_D is calculated. As shown in Fig. 4(a), without tilted plates ($N = 0$, black line), the magnitude of $\langle V_{Ay} \rangle$ is on the order of 10^{-3}, extending over the range from 0.001 to 0.004. The value of $\langle V_{Ay} \rangle$ increases with the value of F_D increasing, indicating the massive velocity loss in the y direction. After embedding the tilted plates ($N = 2$ and 4, red and blue lines, respectively), the value of $\langle V_{Ay} \rangle$ is reduced to a lower magnitude, 10^{-4}, and the velocity fluctuations drop to zero as the drive force increases. Especially for $F_D = 7.5$, we track the trajectory of particles with an initial $y_0 = 12.3$ coordinate after the system has reached an equilibrium state through 1×10^7 time steps. The time-dependent y coordinate of the selected disks with an initial y coordinate is monitored as indicated in Fig. 4(b). The trajectory of y coordinate in the case without tilted plates (black line) presents an oscillating upstate, which implies that there is the drift behavior behind laning phase, while that in the case with tilted plates (red line) is almost a straight line, which indicates that tilted plates can stabilize laning phase by suppressing drifting behavior perpendicular to the driving force.

Figure 5(a) further displays the average lane width $\langle d \rangle$ as a function of F_D for $N = 0$ and 4. For $N = 4$, as the drive force increases, $\langle d \rangle$ gradually declines from $\langle d \rangle \approx 7.0$ to a stable value $\langle d \rangle \approx 2.2$. The related dynamical phases can be simply understood by a competition between three effects: the internal interaction forces between the particles, the interaction between particles and titled plates, and the external driving force. When the driving force is very small, the interaction between particles plays a dominant role, and the system is in phase I. With the driving force increasing, these three effects reach a relatively balanced state,[37,38] where the particles of the same kind gather together and the particles of different kinds are significantly separated from each other, and then the system is in a phase-separated state. However, as the driving force is getting larger and larger, the interaction between particles is not enough to offset the external force, so that the particles tend to be discrete and disordered.[38] In the final stage, as the driving force is much larger than the internal interaction between particles, the external driving force and the guiding of tilted plates accelerate the formation of laining phases. As $5.5 < F_D \leq 7.5$, a well laning-A phase is obtained, uniformly divided into four lanes with $\langle d \rangle \approx 7.0$ as shown in Fig. 3(c). As the value of F_D increases, the influence of tilted plates will diminish and even disappear. For $F_D \geq 17.5$, the two curves for $N = 0$ and 4 basically overlap, illustrating that the system is settled into laning-B phase, irrelevant to the tilted plates. Additionally, even if the tilted plates have no impact on the lane width, it always can stabilize the laning phase as marked by the error bars in Fig. 5(a). Furthermore, the variance of lane width $\langle d^2 \rangle - \langle d \rangle^2$ as a function of N is shown in Fig. 5(b). In the case without tilted plates ($N = 0$), the variance $\langle d^2 \rangle - \langle d \rangle^2$ is in a range between 1.30 and 1.64, and decreases inversely as driving force increases. Once tilted plates are embedded, $\langle d^2 \rangle - \langle d \rangle^2$ drops sharply to 0.2, and even tends to zero for $N = 4$ and 6, independent of the driving force. Moreover, the reduced probability distribution function P of lane width for $F_D = 7.5$ is shown in Fig. 6. Here, the probability distribution $P(\langle d/\langle d \rangle)$ is normalized by $\int P(d/\langle d \rangle)\Delta(\langle d \rangle/\langle d \rangle) = 1/\langle d \rangle$. For the laning phase of $N = 0$, the value of P extends from 0.7 to 1.3, obeying the Gaussian distribution,[39] while for $N = 4$, the value of P is all concentrated at 1.0, following the δ function distribution.[40] These results shown in Figs. 5 and 6 also support the fact that the tilted plates make the laning phase more stable and uniform.

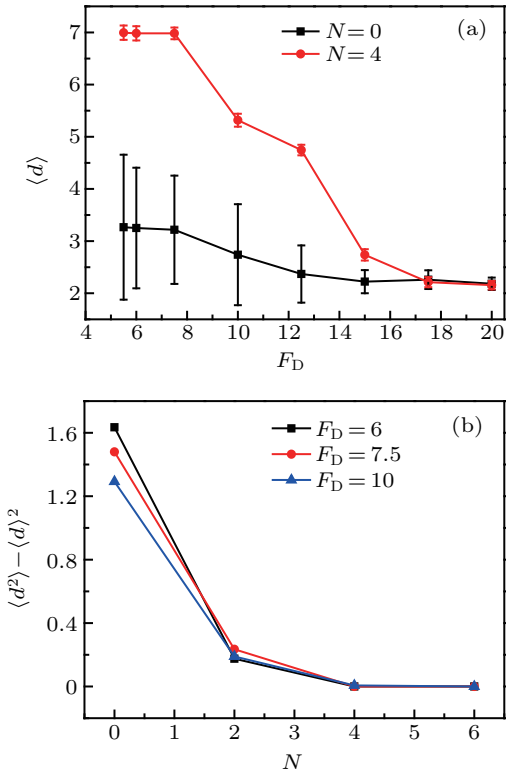


Fig. 5. (a) Average lane width $\langle d \rangle$ as a function of F_D for $N = 0$ and 2, and (b) variance of lane width $\langle d^2 \rangle - \langle d \rangle^2$ as a function of N for $F_D = 6$, 7.5, and 10.

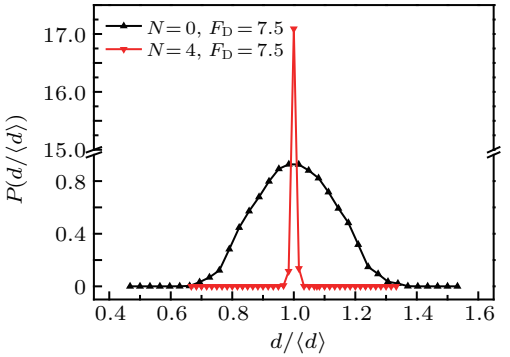


Fig. 6. The reduced probability distribution P with respect to $d/\langle d \rangle$ at $F_D = 7.5$ for $N = 0$ and 4.

According to the results, we can conclude that the tilted plates can effectively govern the collective behaviors of driven particles and then stabilize the laning phase by suppressing drifting behavior perpendicular to the driving force. In this part, we hope to control the lane width distribution freely by varying the interplate distance d_i, not necessarily equal. Figures 7(a1)–7(e1) display the disk configurations for $N = 4$ and $F_D = 7.5$ with different values of d_i, which is characterized by the ratio of $d_1 : d_2 : d_3 : d_4$. The five sets of $d_1 : d_2 : d_3 : d_4$ are selected, which cover the cases of uniform, non-uniform, large differences, and small differences, respectively. Form the configurations, we can make a preliminary judgment that the lane width completely depends on the pre-set interplate distance d_i. Correspondingly, the density profiles of the species A and B along the $+y$ direction are also shown in Figs. 7(a2)–7(e2). The lane width distributions induced by the tilted plates are marked at the top of the density profiles. Taking $d_1 : d_2 : d_3 : d_4 = 1 : 2 : 2 : 1$ for example, the actually measured distance is $1 : 2.067 : 2.070 : 0.989$, which is consistent with the pre-set value.

For $N = 4$ and $F_D = 7.5$, we further change the orientation of the tilted plates from $\theta = 10^\circ$ to $\theta = -10^\circ$, the same uniform laning phases are obtained as shown in Figs. 8(a) and 8(b). The only difference is the order in which the A/B lanes are arranged. As discussed above, the funnel-shaped confinements can first govern the collective behaviors of driven particles from the entrance to the cusp of funnels. As shown in Fig. 8(a), the red disks (species A) driven in the $+x$ direction gather in the third layer characterized by the yellow arrows, while the blue disks (species A) driven in the $-x$ direction gather in the second layer characterized by the red arrows. The time-evolution processes of disk configurations are displayed in Fig. 9. We can see that initially the system is in a fluctuating transient state with disk–disk collisions. Then the funnel-shaped confinements constituted by the neighboring tilted plates govern the collective behaviors of driven particles to the direction of the cusp of funnels. Once driven disks are in a lane (about 1×10^6 time steps), transverse diffusivity is further suppressed and ordered laning phase is formed (after 6×10^6 time steps).

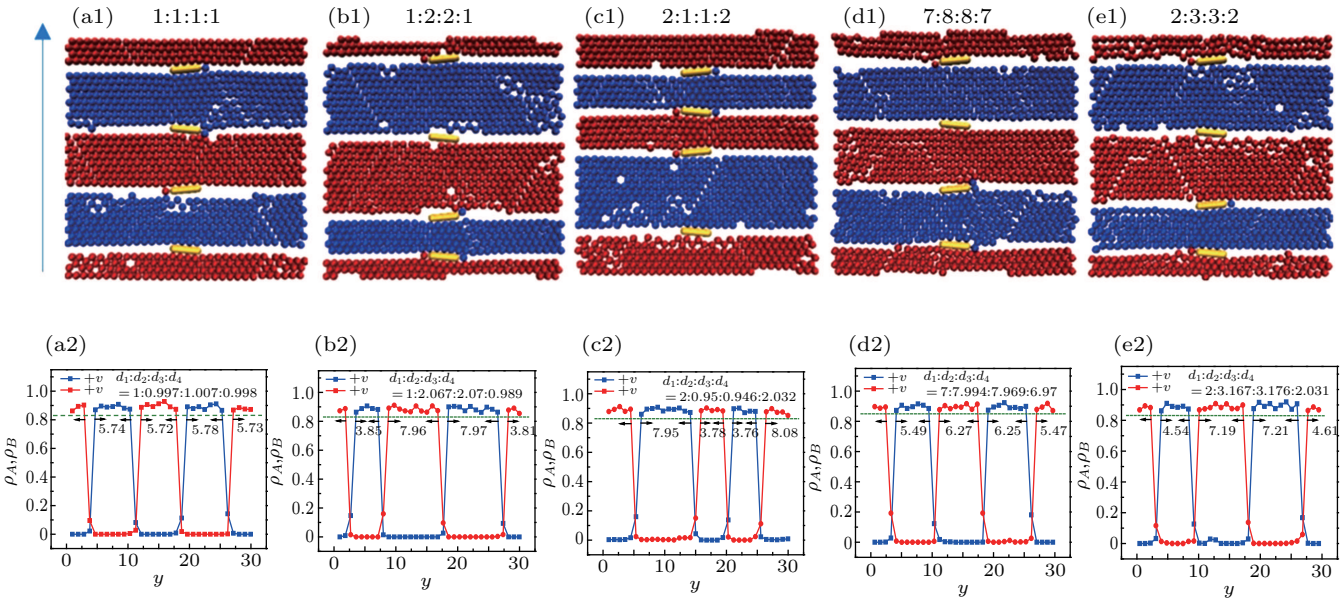


Fig. 7. (a1)–(e1) Disk configurations with different distance ratios of $d_1 : d_2 : d_3 : d_4$ for $F_D = 7.5$ and $N = 4$, and (a2)–(e2) density profiles of species A and B along $+y$ direction.

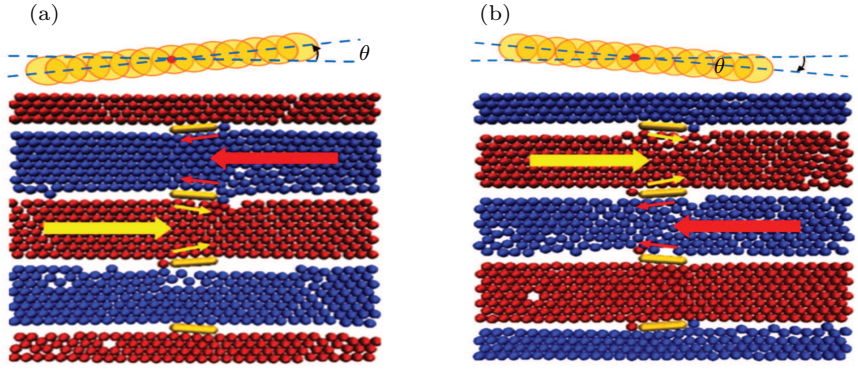


Fig. 8. Disk configuration with tilted angle of $\theta = 10^\circ$ (a) and $\theta = -10^\circ$ (b) for $F_D = 7.5$ and $N = 4$.

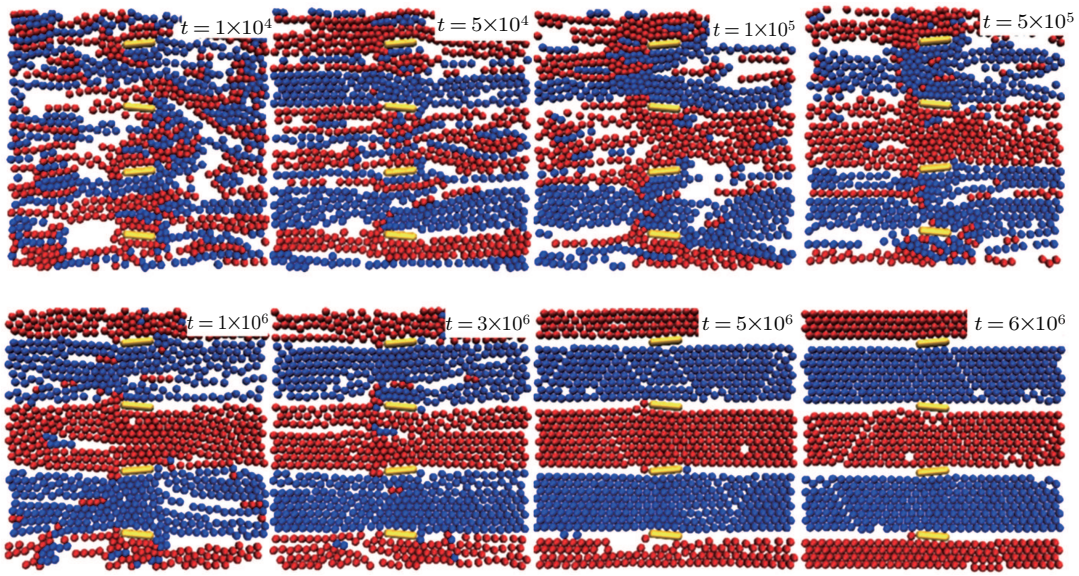


Fig. 9. Time-evolution processes of disk configurations for $F_D = 7.5$ and $N = 4$.

4. Conclusions

We have numerically examined a 2D binary system of particles driven in opposite directions. There are four typical dynamical phases: jammed, phase separated, disordered, and laning states. In general, the dynamical laning phase is unstable with drifting defects and non-uniform lane width distribution, which may impede its wide application in accelerating particle transport. To eliminate drifting defects and control the lane width within laning phase, impermeable tilted plates are introduced into the driven system. We map a rough phase diagram as a function of driving force and plate number. Embedded with tilted plates, the laning phase is stabilized as indicated by a drop both in particle velocity perpendicular to the driving force, and in the variance of lane width. Moreover, the lane width distribution can be controlled freely by the inter-plate distance. We further show that the collective behavior of the particles of the same species s in laning phase can be governed by the funnel-shaped confinements constituted by the neighboring tilted plates. Our results suggest that the embedded tilted plates can serve as an alternative method of stabilizing laning phase and controlling lane width distribution.

References

[1] Cross M C and Hohenberg P C 1993 *Rev. Mod. Phys.* **65** 851
[2] Mikhailov A S and Showalter K 2006 *Phys. Rep.* **425** 79
[3] Katz S, Lebowitz J and Spohn H 1983 *Phys. Rev. B* **28** 1655
[4] Marro J and Dickman R 1999 *Nonequilibrium phase transitions in lattice models* (Cambridge: Cambridge University Press) pp. 50–127
[5] Leunissen M E, Christova C G, Hynninen A P, Royall C P, Campbell A I, Imhof A, Dijkstra M, van Roij R and van Blaaderen A 2005 *Nature* **437** 235
[6] Vissers T, Wysocki A, Rex M, Loewen H, Royall C P, Imhof A and van Blaaderen A 2011 *Soft Matter* **7** 2352
[7] Dzubiella J, Hoffmann G P and Löwen H 2009 *Phys. Rev. E* **79** 021402
[8] Glanz T and Löwen H 2012 *J. Phys.: Condens. Matter* **24** 464114
[9] Klymko K, Geissler P L and Whitelam S 2016 *Phys. Rev. E* **94** 022608
[10] Poncet A, Bénichou O, Démery V and Oshanin G 2017 *Phys. Rev. Lett.* **118** 118002
[11] Morfill G E, Konopka U, Kretschmer M, Rubin-Zuzic M, Thomas H M, Zhdanov S K and Tsytovich V 2006 *New J. Phys.* **8** 7
[12] Sutterlin K R, Wysocki A, Ivlev A V, Rath C, Thomas H M, Rubin-Zuzic M, Goedheer W J, Fortov V E, Lipaev A M and Molotkov V I 2009 *Phys. Rev. Lett.* **102** 085003
[13] Ciamarra M P, Coniglio A and Nicodemi M 2005 *J. Phys.: Condens. Matter* **17** S2549
[14] Jiang R, Helbing D, Shukla P and Wu Q 2006 *Physica A* **368** 567
[15] Kölbl R and Helbing D 2003 *New J. Phys.* **5** 48
[16] Chowdhury D, Nishinari K and Schadschneider A 2004 *Phase Transit.* **77** 601
[17] Wensink H H and Löwen H 2012 *J. Phys.: Condens. Matter.* **24** 464130
[18] Yamao M, Naoki H and Ishii S 2011 *PLoS One* **6** e27950
[19] Jerome Delhommelle 2005 *Phys. Rev. E* **71** 016705
[20] Chakrabarti J, Dzubiella J and Löwen H 2003 *Europhys. Lett.* **61** 415
[21] Chakrabarti J, Dzubiella J and Löwen H 2004 *Phys. Rev. E* **70** 012401
[22] McCandlish R, Aparna Baskaran and Michael F 2012 *Soft Matter* **8** 2527
[23] Reichhardt C and Reichhardt C J O 2018 *Soft Matter* **14** 490
[24] Yang Y, McDermott D, Olson Reichhardt C J and Reichhardt C 2017 *Phys. Rev. E* **95** 042902
[25] McDermott D, Yang Y, Olson Reichhardt C J and Reichhardt C 2019 *Phys. Rev. E* **99** 042601
[26] Reichhardt C, Thibault J, Papanikolaou S and Reichhardt C J O 2018 *Phys. Rev. E* **98** 022603
[27] Reichhardt C and Reichhardt C J O 2017 *Rep. Prog. Phys.* **80** 026501
[28] Bhattacharya S and Higgins M J 1993 *Phys. Rev. Lett.* **70** 2617
[29] Helbing D, Farkas I J and Vicsek T 2000 *Phys. Rev. Lett.* **84** 1240
[30] Braun O M, Dauxois T and Paliy M V 1997 *Phys. Rev. Lett.* **78** 1295
[31] Gutierrez J, Silhanek A V, Van de Vondel J, Gillijns W and Moshchalkov V 2009 *Phys. Rev. B* **80** 140514
[32] Solon A P, Fily Y, Baskaran A, Cates M E, Kafri Y, Kardar M and Tailleur J 2015 *Nat. Phys.* **11** 673
[33] Mijalkov M and Volpe G 2013 *Soft Matter* **9** 6376
[34] Sipos O, Nagy K, Di Leonardo R and Galajda P 2015 *Phys. Rev. Lett.* **114** 258104
[35] Tsiok E N, Dudalov D E, Fomin Yu D and Ryzhov V N 2015 *Phys. Rev. E* **92** 032110
[36] Qi W and Dijkstra M 2015 *Soft Matter* **11** 2852
[37] Redner G S, Hagan M F and Baskaran A 2013 *Phys. Rev. Lett.* **110** 055701
[38] Tung C, Harder J, Valeriani C and Cacciuto A 2016 *Soft Matter* **12** 555
[39] Chen J, Hua Y, Zhou X L and Zhang L X 2017 *Sci. Rep.* **7** 15006
[40] Kaiser A, Sokolov A and Aranson I S 2015 *Eur. Phys. J. Special Topics* **224** 1275